



# Design of a Diagnostic for the Neutral Particle Density Profile Measurement for the TCABR Tokamak



F.A.F. Albuquerque<sup>1</sup>, J.H.F. Severo<sup>2</sup>, N.U. Wetter<sup>1</sup>

<sup>1</sup>Instituto de Pesquisas energéticas e Nucleares IPEN-CNEN, Brazil

<sup>2</sup>Institute of Physics of University of São Paulo, Brazil

Hold at USP, August 28 to September 9, 2023

**Abstract:** This paper summarizes this research project, where it proposes a detailed study focused on implementing a new diagnostic method to measure local densities of neutral particles within the plasma column of the TCABR tokamak. The diagnostic approach relies on Laser Induced Ionization (LII) of excited atoms [1] and the subsequent analysis of the intensity reduction of spectral lines emitted by these atoms due to the ionization. The study involves simulating all the laser optical system in the Ansys Zemax OpticsStudio Software, optimizing laser parameters (wavelength, energy, beam diameter, etc.), and determining the diagnostic's resolution [2]. Utilizing plasma electronic density and temperature profiles of the TCABR tokamak, along with the OPEN-ADAS code (Atomic Data and Analysis Structure), the research will also estimate photoionization coefficients and spectral line intensity reduction for hydrogen, allowing to calculate the atom's density in its ground state within the plasma [3].

## INTRODUCTION

As a laser beam is able to interact with the plasma confined in magnetic systems, it is possible to use the laser to infer the local parameters of that plasma. If the laser produces some reaction (ionization, excitation, etc.) in the atoms or ions that make up the plasma, then it is possible, in real time, to obtain local information on the plasma volume terminated at the crossing of the laser beam with the line of sight joining the detector to the plasma column.

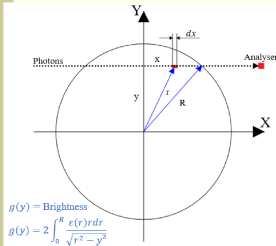


Fig.1 Schematic representation of the measurement of the radiance (brightness) of the plasma column

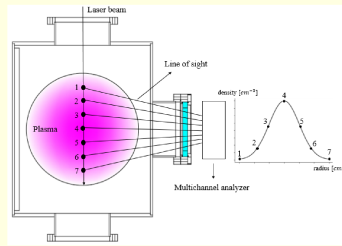


Fig.2 Schematic representation of the emissivity of the plasma column

The Laser Induced Ionization (LII) method consists of the ionization of a population of an atom excited at a certain energy level  $j$  whose transition to level  $i$  occurs through the emission of photons whose wavelength  $\lambda$  depends on the difference in energy between levels  $j$  and  $i$ . During the action of the laser, a reduction in the intensity of the spectral line resulting from the transition  $j \rightarrow i$  is observed. The real-time measurement of this reduction in intensity allows us to infer the population density of the level and therefore the density of that atom in its ground state. Equation (1) shows the temporal evolution of the density of the population at an  $i$  state due to processes of excitation, deexcitation and ionization.

$$\frac{dN_i}{dt} = \sum_{j>i} A_{j,i} N_j - \sum_{j<i} A_{i,j} N_i + \sum_{j>i} n_e N_j \langle \sigma \nu \rangle_{j,i}^{deexc} - \sum_{j<i} n_e N_i \langle \sigma \nu \rangle_{i,j}^{deexc} + \sum_{j>i} n_e N_j \langle \sigma \nu \rangle_{j,i}^{exc} - \sum_{j<i} n_e N_i \langle \sigma \nu \rangle_{i,j}^{exc} + n_e N_i \langle \sigma \nu \rangle_{i,i}^{ion} \quad (1)$$

## DIAGNOSTIC SYSTEM

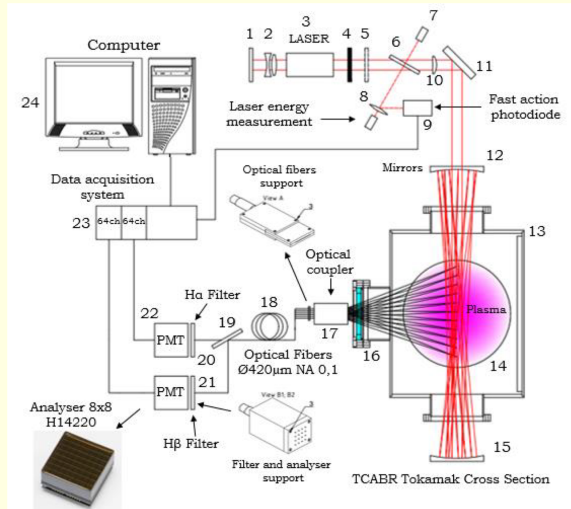


Fig.3 Schematic representation of the Laser-Induced Ionization diagnosis. 1 - Flat rear mirror, 2 - Laser objective, 3 - Laser, 4 - Saturable absorber, 5,6 - Flat glass plates 7,8 - Laser energy measurement system, 9 - Fast action photodiode, 10 - Focusing objective, 11 - Flat mirror, 12,15 - Cavity mirrors, 13 - Cross section of the TCABR Tokamak, 14 - Plasma column, 16 - Equatorial window, 17 - Optical coupler, 18 - Optical fiber set, 19 - Semi-Mirror, 20 - H $\alpha$  filter, 21 - H $\beta$  filter, 22 - Multichannel PMT detectors, 21 - DAS, 22 - Computer.

## RESULTS

The LII diagnostic must operate in a regime where the rate of ionization produced by the beam must be independent of the laser energy density. This operating regime is called saturated, that is, the reduction in the excited state population must be essentially independent of the probing laser intensity.

The quantity of most interest is the ratio of the reduction of the population at an upper state  $j$  with the laser action. Equation 2 shows the relation of the reduction of the population in function of the laser flux  $\Phi(\nu_L)$  and the so-called laser saturation flux  $\Phi_S(\nu_L)$ :

$$\frac{\Delta n_j}{n_j} = \frac{\Phi(\nu_L)}{\Phi_S + \Phi(\nu_L)} \quad \Phi_S(\nu_L) = \frac{h\nu_L}{\tau\sigma_j(\nu)} \quad (2)$$

Tab.1 below shows the calculation of the saturation flux for different types of laser for the transitions of hydrogen  $4 \rightarrow 2$  responsible for the emission of the H $\beta$  spectral line and  $3 \rightarrow 2$  responsible for the emission of the spectral line of H $\alpha$  from the Balmer series. Figures 4 and 5 show the ratio of excited state population reduction as a function of laser saturation flux for H $\beta$  and H $\alpha$  transitions. Tells us to what beam intensity all excited atoms in level  $j$  are ionized.

H $\beta$ :  $4 \rightarrow 2$

Laser	$\nu_L$ [s <sup>-1</sup> ]	$\lambda_L$ [nm]	$R_L$ [J]	$h$ [J.s]	$\sigma_j(\nu)$ [m <sup>2</sup> ]	$\tau_j$ [s]	$\Phi_S$ [MW/cm <sup>2</sup> ]
Ruby	$4.32 \cdot 10^{14}$	694,3	$2.18 \cdot 10^{-18}$	$6.63 \cdot 10^{-34}$	$5.92 \cdot 10^{-22}$	$37 \cdot 10^{-9}$	1,31
Nd-YAG	$2.82 \cdot 10^{14}$	1061	$2.18 \cdot 10^{-18}$	$6.63 \cdot 10^{-34}$	$2.13 \cdot 10^{-21}$	$37 \cdot 10^{-9}$	0,24
He-Ne	$4.74 \cdot 10^{14}$	632,8	$2.18 \cdot 10^{-18}$	$6.63 \cdot 10^{-34}$	$4.48 \cdot 10^{-22}$	$37 \cdot 10^{-9}$	1,90

H $\alpha$ :  $3 \rightarrow 2$

Laser	$\nu_L$ [s <sup>-1</sup> ]	$\lambda_L$ [nm]	$R_L$ [J]	$h$ [J.s]	$\sigma_j(\nu)$ [m <sup>2</sup> ]	$\tau_j$ [s]	$\Phi_S$ [MW/cm <sup>2</sup> ]
Ruby	$4.32 \cdot 10^{14}$	694,3	$2.18 \cdot 10^{-18}$	$6.63 \cdot 10^{-34}$	$2.49 \cdot 10^{-21}$	$15 \cdot 10^{-9}$	0,77
Nd-YAG	$2.82 \cdot 10^{14}$	1061	$2.18 \cdot 10^{-18}$	$6.63 \cdot 10^{-34}$	0	$15 \cdot 10^{-9}$	0
He-Ne	$4.74 \cdot 10^{14}$	632,8	$2.18 \cdot 10^{-18}$	$6.63 \cdot 10^{-34}$	$1.89 \cdot 10^{-21}$	$15 \cdot 10^{-9}$	1,11

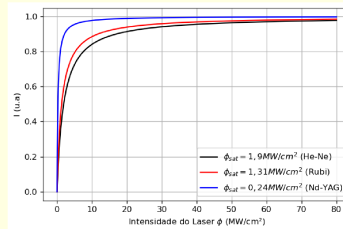


Fig.4 Laser saturation flux for the dependency of the ratio  $\Delta n_j/n_j$  over the transition H $\beta$

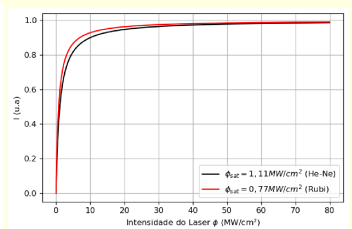


Fig.5 Laser saturation flux for the dependency of the ratio  $\Delta n_j/n_j$  over the transition H $\alpha$

The brightness shown in the Figure 1 is a function of the Photon emissivity coefficients (PECs) for the processes of excitation, recombination and thermal charge exchange.

$$\epsilon_{jk} = \xi_{exc} n_e n_z + \xi_{rec} n_e n_{z+1} + \xi_{cx} n_H n_{z+1} \quad (3)$$

PECs were obtained from the OPEN-ADAS code for the Balmer series and are shown at Figures 6, 7 and 8.

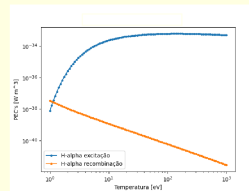


Fig.6 Excitation and Recombination PECs for the transition H $\alpha$

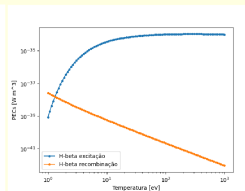


Fig.7 Excitation and Recombination PECs for the transition H $\beta$

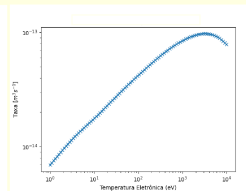


Fig.8 Thermal charge Exchange rate for Hydrogen

## REFERENCES

- [1] V. I. Gladushchak et al - Nucl. Fusion 35 (1995), 1385–1390.
- [2] M.Yu.Kantor et al - 13th International Symposium on Laser-Aided Plasma Diagnostics (2007), 18-21.
- [3] E. Panarella - Foundations of Physics, Vol. 4, No. 2, 1974.